Decellularized porcine dermis as material in blended bioink for 3D bioprinting

Nghia Thi Hieu Phan[1,2,3], Ha Le Bao Tran[1,2,3*], Nhan Thuc Chi Ha[3,4], Anh Nguyen Ngoc Bui[2,3] and My Thi Ngoc Nguyen[1,2,3]

1. Laboratory of Tissue Engineering and Biomedical Materials, University of Science, Ho Chi Minh City, VIETNAM
2. Department of Physiology and Animal Biotechnology, Faculty of Biology and Biotechnology, University of Science, Ho Chi Minh City, VIETNAM
3. Vietnam National University, Ho Chi Minh City, VIETNAM
4. Faculty of Materials Science and Technology, University of Science, VNU-HCM, Ho Chi Minh City, VIETNAM
*tlbha@hcmus.edu.vn

Abstract

Decellularized extracellular matrix (dECM) derived from porcine dermis has emerged as a promising biomaterial for bioink development in tissue engineering. The purpose of this study was to fabricate the porcine dermal ECM-based bioink and to evaluate its printability as well as cytotoxicity. The bioink was prepared by decellularizing porcine dermis, processing it into a solution and blending with gelatin and alginate. The decellularization effectively was determined using histological staining (Hematoxylin and Eosin), DNA quantification and electrophoresis. Additionally, retention of key ECM proteins, including collagen and elastin, was confirmed by Masson's Trichrome and Van Gieson's staining. Printability was assessed by inversion test, filament formation and pore printability index (Pr). Cytotoxicity was evaluated using L929 cells. The results demonstrated efficient decellularization, with complete removal of cellular components and minimal residual DNA content (≤ 50 ng/mg ECM, without detectable DNA fragments of ≥ 200 bp).

Furthermore, the bioink retained essential ECM proteins such as collagen and elastin. The bioink exhibited excellent printability, forming stable filaments and achieving a high pore printability index (Pr = 0.97 ± 0.010). Cytotoxicity tests confirmed that the bioink was non-toxic to L929 cells. These findings suggest that dECM-based bioinks hold significant potential for 3D bioprinting applications in tissue engineering.

Keywords: 3D bioprinting, bioink, decellularized extracellular matrix, porcine dermis, tissue engineering.

Introduction

Tissue engineering is a fast emerging science that attempts to build functioning tissues and organs to address the rising need for organ transplants and advances in regenerative medicine[8]. The basis of this strategy is the creation of biomaterials that closely resemble the extracellular matrix (ECM), a complex of proteins and polysaccharides that offer structural and biochemical support to cells[28]. Decellularized ECM from natural sources has gained attention for its ability to mimic the native tissue microenvironment, promoting essential cellular functions for tissue regeneration[7,30]. Among the various sources of ECM, porcine dermis is particularly promising due to its compositional and structural similarities to human dermal ECM, making it an ideal candidate for bioink formulations in tissue engineering[15,18].

The decellularization method successfully eliminates cellular components while retaining the ECM's architecture and bioactive chemicals, yielding a biocompatible scaffold suitable for cell attachment, proliferation and differentiation[3]. Bioprinting, a cutting-edge additive manufacturing process, enables the exact positioning of cells and biomaterials, permitting the production of complex, structurally defined tissue constructions[1,27]. However, a major challenge lies in developing bioinks that possess appropriate printability properties and biocompatibility for successful bioprinting[1,19,27].

Combining dECM with biopolymers such as gelatin and alginate can enhance the bioink's mechanical properties, printability and cell compatibility[29]. Gelatin, derived from collagen, provides bioactivity and thermal responsiveness, while alginate, a natural polysaccharide, contributes to structural stability and shape fidelity upon cross-linking[5,21]. Therefore, this study explores the potential of incorporating dECM from porcine dermis into bioink formulations for 3D bioprinting. By blending dECM with gelatin and alginate, we aim to develop bioinks that replicate the native tissue environment, improving printability and biocompatibility. This approach holds promises for enhancing the development of functional tissue constructions, providing innovative solutions for regenerative medicine and advancing the science of tissue engineering.

Material and Methods

Decellularization of porcine dermal tissue: Full-thickness porcine skin samples were collected at a nearby slaughterhouse and delivered to the laboratory within 1 - 2 hours after collection. The samples were thoroughly rinsed with distilled water to eliminate surface contaminants and debris. The epidermis and hypodermis were then removed, leaving the isolated dermal layer (Fig. 1) which was subsequently cut into smaller sections of approximately 1 cm × 1 cm for the decellularization process. The porcine dermis was decellularized using a modified version of the protocol described by Reing et al[17].

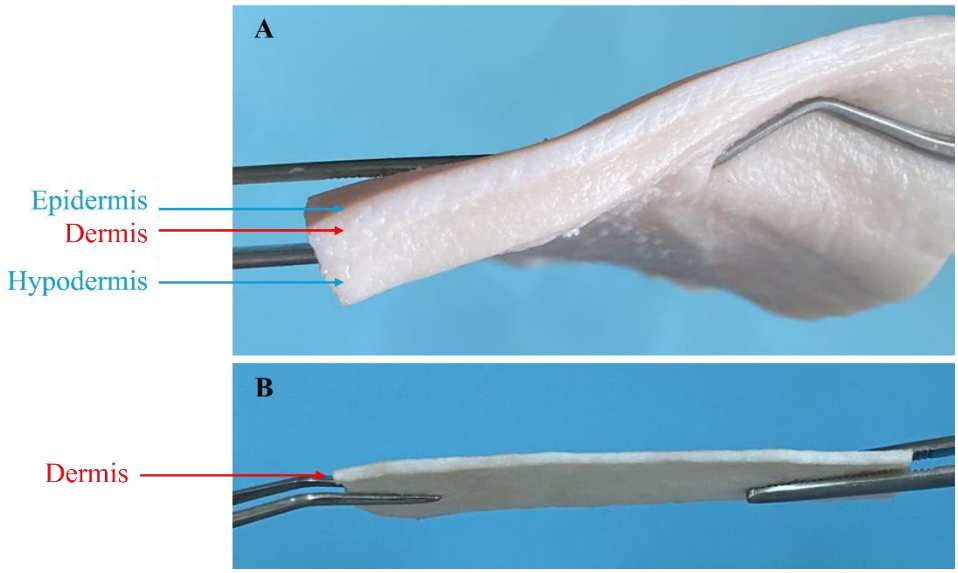

Figure 1: Porcine skin samples before and after processing
A – Porcine skin sample after cleaning, before processing, B – Porcine skin sample after processing, with the epidermis and hypodermis removed, leaving only the dermal layer.

The samples were treated with 0.1% sodium dodecyl sulfate (SDS; Sigma) for 24 hours, followed by 1% Triton X-100 (Sigma) combined with 0.1% ammonium hydroxide (NH_4OH; Merck) for another 24 hours and finally, 100% isopropanol (Merck) for 2 hours. After each treatment step, the samples were washed with distilled water at 90 rpm for 45 minutes to ensure the removal of residual chemicals. After each treatment stage, the samples were rinsed with distilled water at 90 rpm for 45 minutes to remove any remaining contaminants.

Assessment of decellularization efficiency: The decellularization efficiency of dermis samples was evaluated based on three criteria: (1) the lack of visible cells observed in Hematoxylin and Eosin (H and E) staining, (2) residual DNA content was determined through DNA extraction using the Genelute™ kit (Sigma), with DNA concentration measured at 260 nm using a NanoDrop spectrophotometer (Thermo Scientific) and (3) the size of the remaining DNA fragments was analyzed via electrophoresis on a 2% agarose gel.

Assessment of dECM components - collagen and elastin: The presence of collagen and elastin in the dECM was confirmed through Masson's Trichrome and Van Gieson's staining. First, samples were fixed in formalin, embedded in paraffin and sectioned into 3-5 µm thick slices. The sections were then deparaffinized and stained with Masson's Trichrome to visualize collagen fibers. Van Gieson's stain was applied to specifically highlight elastin fibers. The stained sections were examined under a light microscope, confirming the presence and distribution of collagen and elastin based on their distinct coloration.

Preparation of dECM solution: The dECM samples were initially frozen at -86°C overnight, followed by freeze-drying using a lyophilizer (SP Scientific) for 6 hours to completely remove water content. The dried ECM was then sterilized using 25 kGy of gamma irradiation. Subsequently, the dECM was finely minced and dissolved in a pepsin solution (1 mg/mL in 0.01N HCl) (Sigma). This dissolution process was conducted under continuous stirring on a magnetic stirrer at room temperature for 24 hours, protected from light. The dissolved dECM solution was then neutralized on ice with 0.1N NaOH (Merck) and supplemented with 10X phosphate-buffered saline (PBS; Gibco) to achieve a physiological pH, resulting in a final dECM concentration of 10 mg/mL.

Formulation of dECM-based bioink: The dECM-based bioink was formulated by blending the dECM solution with gelatin (Sigma) and alginate (Sigma). Initially, the gelatin-alginate solution and 0.07M calcium chloride ($CaCl_2$, Merck) solution were prepared and sterilized by autoclaving at 121°C for 15 minutes. Following sterilization, the $CaCl_2$ solution was gradually added to the gelatin-alginate mixture while stirring continuously to ensure thorough mixing. Subsequently, the dECM solution was introduced into this mixture and stirring continued until a homogeneous blend was achieved. The final concentrations of the components in the bioink are: 4% (w/v) gelatin, 4% (w/v) alginate, 1% (w/v) ECM and 14mM $CaCl_2$ (prepared from a 0.07M $CaCl_2$ stock solution at 20% v/v). The prepared bioink was then transferred into 3 mL syringes (Becton, Dickinson and Company) and stored at 4°C until further use.

Printability of dECM-based bioink: The printability of the dECM-based bioink was assessed through inversion test, filament formation and pore printability.

Inversion test: Two milliliters of bioink were transferred into a 5 mL vial. The vial was inverted and allowed to remain stable for 30 minutes to observe gelation status of bioink.

Filament formation: The bioink was loaded into a 3 mL syringe and extruded using a BIO X 3D bioprinter (Cellink). The formation of filaments in the air was recorded using a camera.

Pore printability (Pr): For pore printability, the bioink was again loaded into a 3 mL syringe and printed using the BIO X 3D bioprinter according to the model in fig. 2. The printed products were recorded and ImageJ software was utilized to analyze and measure the perimeter and area of the pores. The Pr value was calculated using equation (1)[16]:

$$\mathrm{Pr} = \frac{L^2}{16 \times A} \quad (1)$$

where Pr is the pore printability, L is the perimeter of the pore and A is the area of the pore.

Cytotoxicity of dECM-based bioink: Cytotoxicity was assessed according to ISO 10993-5 using L929 mouse fibroblasts (ATCC)[22]. The bioink was immersed in a media for cell culture consisting of DMEM/F12, enriched with 10% fetal bovine serum (FBS) and 1% penicillin/streptomycin. The extracts were collected following a 24-hour incubation period at 37°C, as ISO 10993-12 guidelines. In a 96-well plate, the L929 cells were seeded at a density of 10^4 cells/well and exposed to 100 µL of each extract. For control purposes, a medium for cell culture was used as a negative control and 20% DMSO was employed as a positive control. Following a 24-hour incubation at 37°C with 5% CO_2, the medium was discarded from each well and 100 µL of 3-(4,5-dimethylthiazol-2-yl)-2,5-diphenyl tetrazolium bromide (MTT) solution (0.5 mg/mL, Sigma) was then added.

The plate underwent incubation in the dark at 37°C with 5% CO_2 for a duration of 4 hours. The MTT solution was subsequently removed and 100 µL of a DMSO/EtOH solution was added to dissolve the formazan crystals. Absorbance was quantified at 570 nm utilizing a microplate reader. The relative growth rate (%RGR) was determined using equation (2):

$$RGR\ \% = \frac{100 \times OD_{570a}}{OD_{570b}}\ x\ 100\% \quad (2)$$

where OD_{570a} is the optical density of the extract-treated group and OD_{570b} is the optical density of the negative control group.

Statistical analysis: Image J and Excel were used to handle experimental data; statistical analyses were performed using GraphPad Prism version 9.0 (GraphPad, San Diego, CA, USA). To evaluate the distinctions between the groups, ANOVA was implemented. In order to guarantee reliability, all experiments were conducted at least three times and the results were reported as means ± standard deviations. Statistical significance was established by calculating a p-value of ≤ 0.05.

Results and Discussion

Efficiency of decellularization: The efficiency of decellularization of dermis samples was evaluated through H and E staining for cell absence and the analysis of residual DNA content and fragment size, with native dermis as the control. In the native dermis sample, numerous purple-blue spots, representing residual cells, were observed. In contrast, the dECM exhibited no such staining, indicating successful removal of cellular components. The ECM structure in the decellularized sample retained its pink-stained appearance, similar to the native dermis, suggesting that the decellularization process did not significantly disrupt the ECM structure (Fig. 3A).

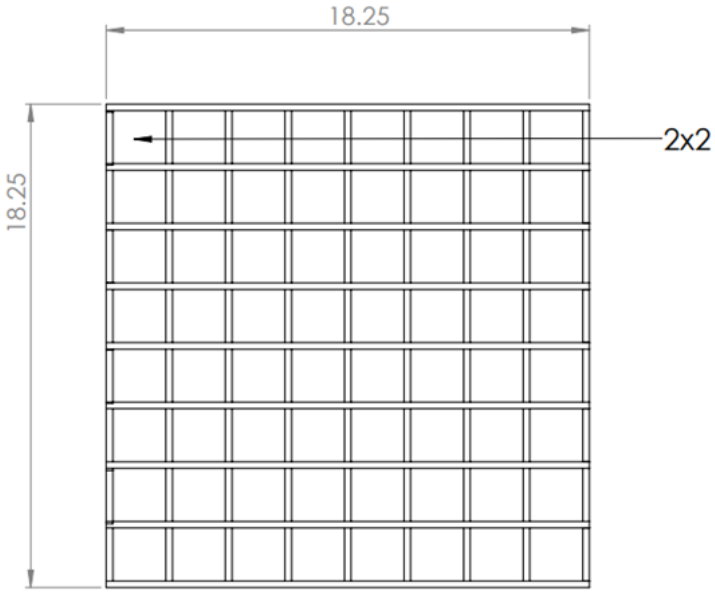

Figure 2: Pore printability assessment model (unit: mm)

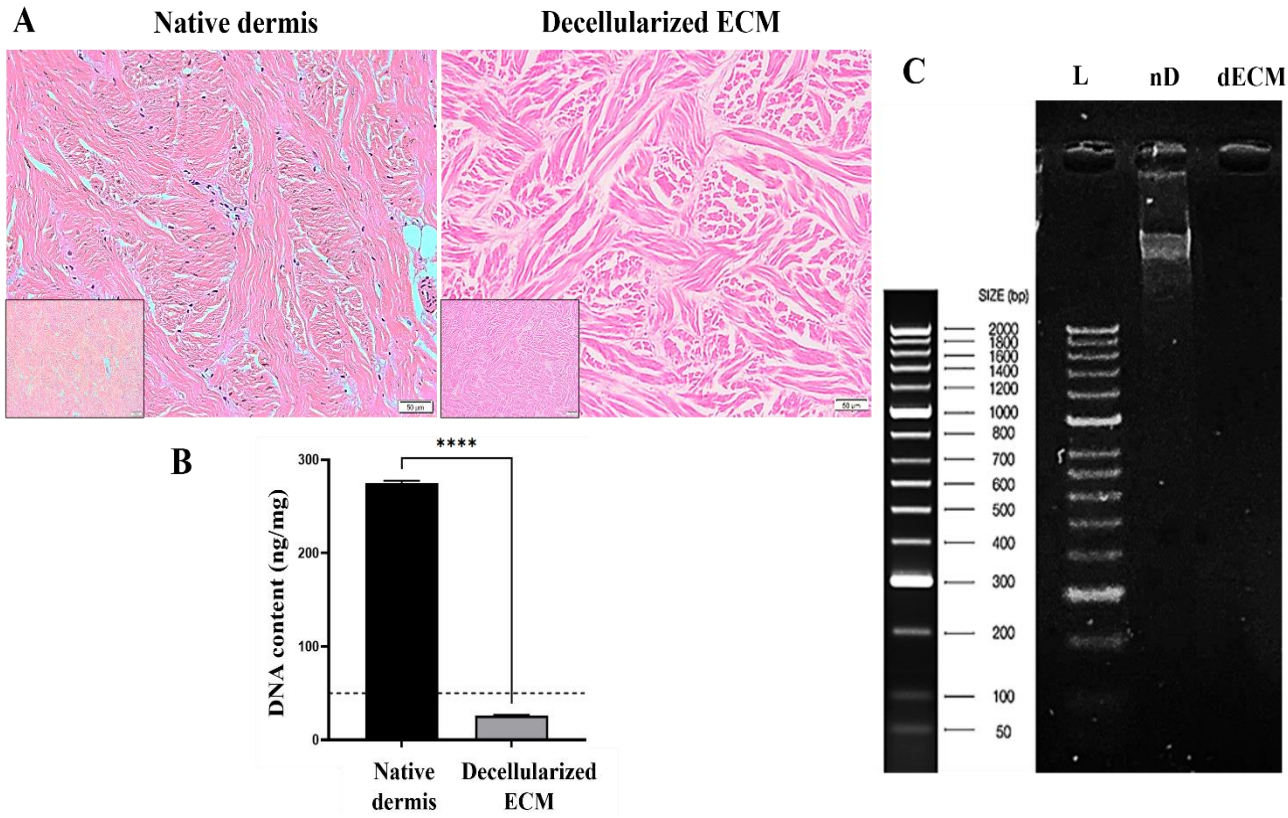

Figure 3: Decellularization Efficiency of Porcine Dermal ECM
A – H and E staining results showing residual cells in the samples, B – DNA content remaining in the samples (**: $p \leq 0.0001$), C – DNA electrophoresis results for ECM samples (L: ladder 50 bp, nD: native dermis, dECM: decellularized ECM)**

The findings of this study are consistent with previous research by Reing et al[17], Wolf et al[26] and Lee et al[14], demonstrating the effectiveness of the decellularization process in removing cellular components from tissue samples. This study proposes a decellularization protocol that utilizes fewer chemicals and significantly reduces processing time while maintaining effective cellular removal. Specifically, the protocol established by Reing et al[17] employed a combination of chemicals including 0.25% trypsin, 70% ethanol, 3% H_2O_2, 0.1% SDS, 1% Triton X-100 and peracetic acid in a Tris-EDTA buffer. Similarly, Wolf et al[26] utilized a protocol that included 0.25% trypsin, 70% ethanol, 3% H_2O_2 and 1% Triton X-100, along with additional reagents.

The method developed by Lee et al[14] focused primarily on 1% Triton X-100 supplemented with 0.1% ammonium hydroxide; however, this process required over five days to achieve decellularization. In contrast, the decellularization protocol employed in this study demonstrated a shorter processing time (over two days) and reduced chemical exposure, effectively preserving the integrity of the ECM. Three primary chemicals for decellularization including 0.1% SDS, 1% Triton X-100 and 100% isopropanol were used. SDS is an ionic detergent that effectively breaks protein-protein bonds, facilitating the removal of cellular proteins and nuclear materials. Hashemi et al[9] observed that extending the treatment duration with SDS leads to a reduction in cell numbers and enhances decellularization effectiveness; however, this may negatively impact the structures of the ECM.

Consequently, SDS is applied at a low concentration (0.1%) to limit its effects on the ECM architecture. However, SDS can alter ECM structure, especially proteins like collagen. While SDS excels in removing cytoplasmic proteins and antigens, any residual detergent can lead to inflammation and cytotoxic effects, hindering tissue recellularization. Therefore, thorough rinsing of SDS is necessary. Triton X-100, a non-ionic detergent, complements SDS by helping to remove residual amounts while preserving ECM integrity. Although it can disrupt lipid and DNA-protein bonds, it largely spares collagen. However, high concentrations of Triton X-100 may reduce GAGs, laminin and fibronectin, though its impact is less severe than that of ionic detergents[11].

Additionally, Triton X-100 can be combined with NH_4OH in several studies on decellularization of animal tissues. For example, research by Baptista et al[2] demonstrated that using a combination of 1% Triton X-100 and 0.1% NH_4OH removed up to 97% of DNA while preserving key proteins like collagen.

In addition to the removal of cells, it is crucial to also eliminate residual materials such as lipids from adipose

tissue and cell membranes. Isopropanol is commonly used to aid in the removal of lipids from tissues[4]. The non-polar carbon chains in these alcohols facilitate the solubilization of non-polar substances including lipids[12]. Moreover, significant protein components can remain intact in the ECM when treated with isopropanol, which reduces the influence of surfactants on protein levels during the decellularization process. Isopropanol not only removes both cells and lipids effectively but also preserves a higher concentration of ECM proteins[25].

Regarding the DNA content, the control sample exhibited a DNA concentration of 274.63 ± 2.95 ng/mg dry weight, while the decellularized sample contained only 26.44 ± 0.42 ng/mg dry weight (Fig. 3B). A significant reduction in DNA levels was noted following the decellularization process, resulting in a statistically significant difference between the two groups ($p \leq 0.0001$). Gel electrophoresis also provided additional validation of these results by demonstrating the absence of detectable DNA bands in the decellularized sample, whereas the native dermis exhibited DNA bands larger than 2000 bp (Fig. 3C). These results demonstrate that the decellularization process was highly effective in removing both cellular material and residual DNA from the samples. Given that DNA is a component of cellular nuclei and can induce immune responses in grafts, reducing DNA levels to below 50 ng/mg dry weight and fragment sizes to less than 200 bp is crucial[4,17].

The results indicate that the decellularization process effectively removed residual DNA, thereby minimizing the risk of immune reactions when used in clinical applications.

dECM components: collagen and elastin: The evaluation of residual collagen and elastin in dECM samples, as revealed by Masson's Trichrome and Verhoeff-van Gieson staining, demonstrates the retention of both components. Collagen fibers, which stain blue, are present in dense, interwoven networks throughout both native and decellularized samples (Fig. 4). Although some fragmentation of collagen fibers occurs in the decellularized samples due to the processing, the overall structure remains similar to that of the native dermis. Elastin fibers, which stain black or near black, are also preserved in the dECM. Native dermis displays intact, densely packed elastin fibers while the dECM shows some fiber loosening and lighter staining, resulting from the decellularization process.

Despite these changes, elastin remains detectable in the decellularized samples. Collagen and elastin are critical structural proteins in the ECM of dermal tissue, providing essential mechanical support and elasticity[13]. Collagen, which constitutes 77% of the non-fat weight of human skin, is crucial for tensile strength and structural integrity, while elastin contributes to tissue elasticity[6,23,24]. The decellularization process effectively removes cellular components and DNA while retaining these vital ECM proteins, making the dECM suitable for bioink applications.

Printability of dECM-based bioink: After the mixing process, the bioink exhibited a gel-like consistency and retained its shape stably for up to 30 minutes inversion (Fig. 5A). This stability is crucial as it enhances the bioink's ability to print complex structures and supports cell encapsulation[20]. Evaluation of filament formation revealed that the bioink successfully extruded continuous and straight filaments from the nozzle to the printing surface (Fig. 5B). The pore printability (Pr) index was measured at 0.97 ± 0.010 which is close to 1 (Fig. 5C), indicating effective pore structure replication[16].

Additionally, the bioink produced square-shaped pores with excellent shape retention and uniform dimensions. The tight molecular bonds within the bioink facilitated precise pore printing, maintaining structural integrity and model fidelity, consistent with previous research[10,16]. These findings suggest that bioink is well-suited for printing multi-layered and complex structures.

Cytotoxicity of ECM-based bioink (Fig. 6): Cell toxicity is a critical assessment for ensuring the safety and potential biomedical application of materials. The cytotoxicity evaluation was conducted using the L929 cell line following ISO 10993-5 standards[22]. The results indicate that the negative control (cells treated with complete culture medium) exhibited a high cell viability rate with a %RGR of 100%. In contrast, the positive control (cells treated with 20% DMSO solution) displayed significantly reduced cell viability, with a %RGR of 12.27 ± 1.545%. According to ISO10993-5 standards, a %RGR value below 70% suggests cytotoxicity[22]. The bioink sample demonstrated a %RGR of 94.68 ± 3.042%, which is well above the 70% threshold, indicating that the bioink does not exhibit cytotoxic effects.

These results indicate that potentially toxic chemicals from the decellularization process have been effectively removed, or that any remaining residues are minimal to harm the cells. This finding is consistent with theoretical expectations, as this ECM-based bioink formulation was made from gelatin, alginate and dECM, which come from natural materials known to support cell proliferation[27].

Future studies should focus on evaluating the long-term viability and functionality of cells encapsulated in the bioink, particularly their behavior in various physiological conditions. Additionally, varying the concentrations of alginate and gelatin may provide important insights for optimizing the bioink formulation, ultimately enhancing its effectiveness in biomedical applications.

Conclusion

This study successfully demonstrated the use of decellularized porcine dermis as a material in a blended bioink for 3D bioprinting, showcasing its promising printability and biological properties suitable for tissue engineering applications. The decellularization process effectively removed cellular components, achieving a

minimal residual DNA content of ≤ 50 ng/mg ECM, with no detectable DNA fragments of ≥ 200 bp while essential ECM proteins, including collagen and elastin, were preserved.

The formulated bioink exhibited excellent printability, characterized by stable filament formation and a high pore printability index (Pr = 0.97 ± 0.010) indicating its suitability for 3D bioprinting applications. Additionally, cytotoxicity assessments using L929 cells confirmed that the bioink was non-cytotoxic. These findings suggest that bioinks derived from decellularized porcine dermis hold significant potential for the development of advanced bioinks in regenerative medicine and tissue engineering.

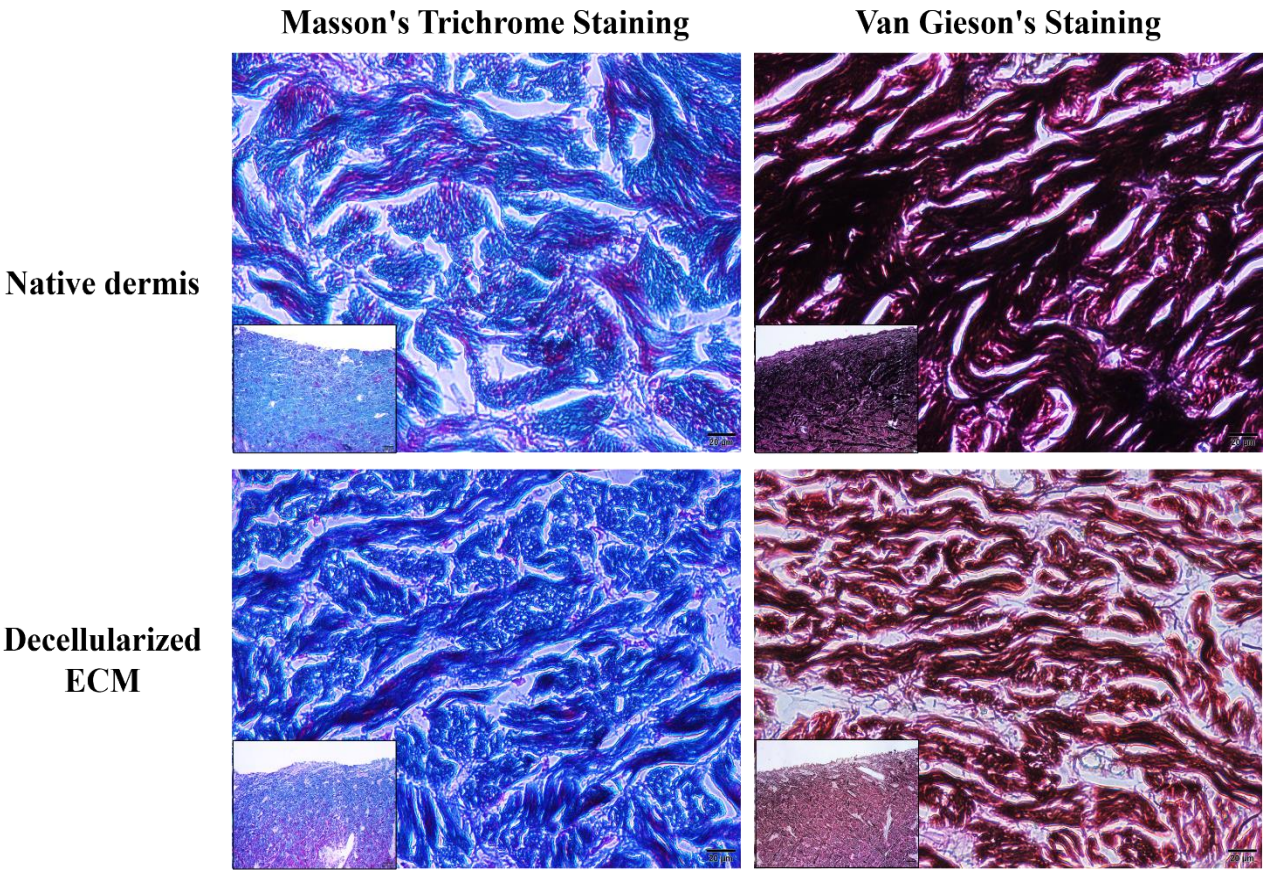

Figure 4: Masson's Trichrome Staining (Collagen) and Van Gieson's Staining (Elastin) of dECM

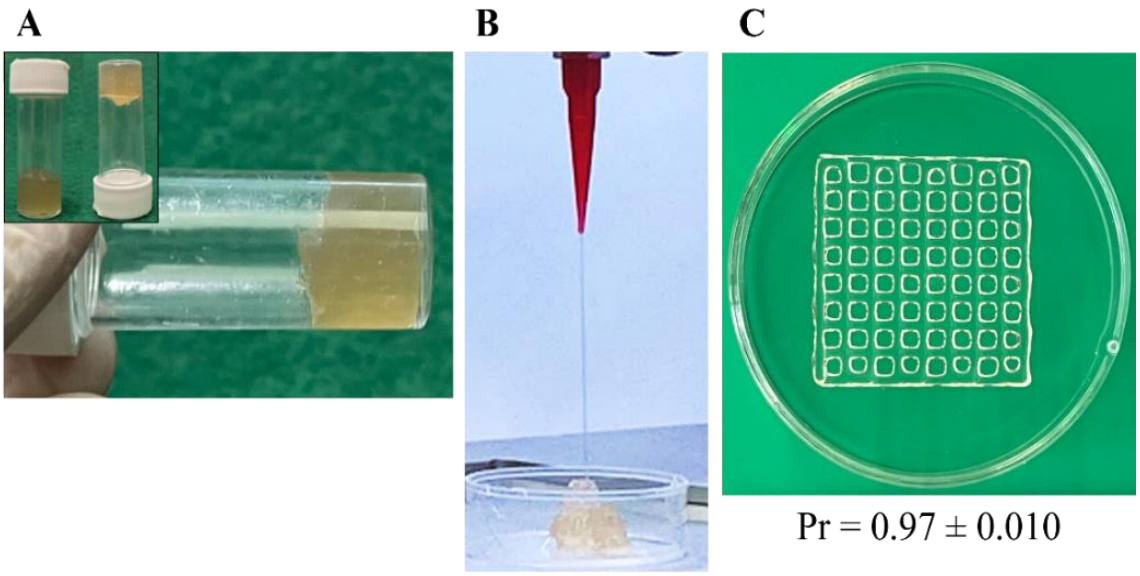

Figure 5: Printability of dECM-based bioink
A – Gelation status of the dECM-based bioink, B – Formation of filaments from the bioink, C - Pore printability (Pr) value of the bioink

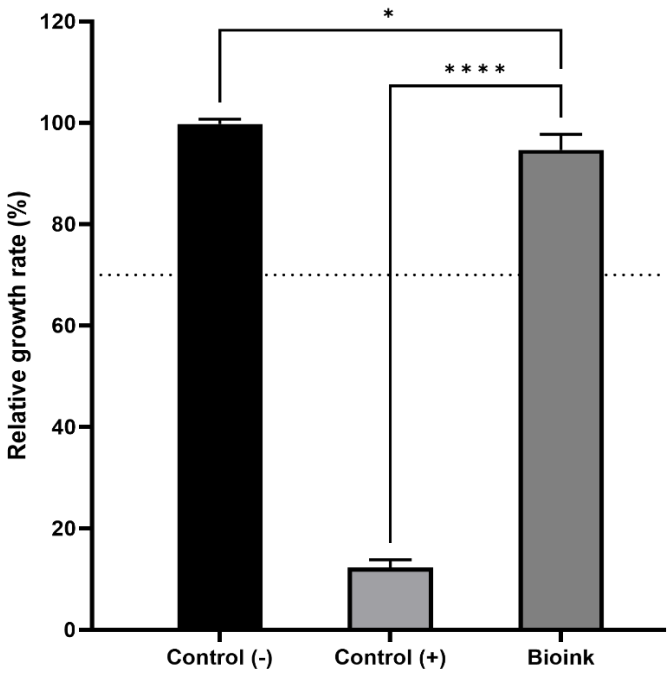

Figure 6: The relative growth rate of cells in the dECM-based bioink
***: p ≤ 0.05; ****: p ≤ 0.0001**

Acknowledgement
This research is funded by Vietnam National University, Ho Chi Minh City (VNU-HCM) under grant number B2023-18-09.

References
1. Agarwal S., Saha S., Balla V.K., Pal A., Barui A. and Bodhak S., Current Developments in 3D Bioprinting for Tissue and Organ Regeneration–A Review, *Frontiers in Mechanical Engineering*, **6**, 589171 **(2020)**

2. Baptista P.M., Siddiqui M.M., Lozier G., Rodriguez S.R., Atala A. and Soker S., The use of whole organ decellularization for the generation of a vascularized liver organoid, *Hepatology*, **53(2)**, 604-617 **(2011)**

3. Brown B.N. and Badylak S.F., Extracellular matrix as an inductive scaffold for functional tissue reconstruction, *Translational Research*, **163(4)**, 268-285 **(2014)**

4. Crapo P.M., Gilbert T.W. and Badylak S.F., An overview of tissue and whole organ decellularization processes, *Biomaterials*, **32(12)**, 3233-3243 **(2011)**

5. Fang W., Yang M., Wang L., Li W., Liu M., Jin Y., Wang Y., Yang R., Wang Y., Zhang K. and Fu Q., Hydrogels for 3D bioprinting in tissue engineering and regenerative medicine: Current progress and challenges, *Int J Bioprint*., **9(5)**, 759 **(2023)**

6. Frantz C., Stewart K.M. and Weaver V.M., The extracellular matrix at a glance, *J Cell Sci*., **123(Pt 24)**, 4195-200 **(2010)**

7. Golebiowska A.A., Intravaia J.T., Sathe V.M., Kumbar S.G. and Nukavarapu S.P., Decellularized extracellular matrix biomaterials for regenerative therapies: Advances, challenges and clinical prospects, *Bioactive Materials*, **32**, 98-123 **(2024)**

8. Han F., Wang J., Ding L., Hu Y., Li W., Yuan Z., Guo Q., Zhu C., Yu L., Wang H., Zhao Z., Jia L., Li J., Yu Y., Zhang W., Chu G., Chen S. and Li B., Tissue Engineering and Regenerative Medicine: Achievements, Future and Sustainability in Asia, *Front Bioeng Biotechnol*., **8**, 83 **(2020)**

9. Hashemi S.S., Jowkar S., Mahmoodi M., Rafati A.R., Mehrabani D., Zarei M. and Keshavarzi A., Biochemical Methods in Production of Three-Dimensional Scaffolds from Human Skin: A Window in Aesthetic Surgery, *World J Plast Surg*., **7(2)**, 204-211 **(2018)**

10. Hiller T., Berg J., Elomaa L., Röhrs V., Ullah I., Schaar K., Dietrich A.C., Al-Zeer M.A., Kurtz A., Hocke A.C., Hippenstiel S., Fechner H., Weinhart M. and Kurreck J., Generation of a 3D Liver Model Comprising Human Extracellular Matrix in an Alginate/Gelatin-Based Bioink by Extrusion Bioprinting for Infection and Transduction Studies, *International Journal of Molecular Sciences*, **19(10)**, 3129 **(2018)**

11. Kasravi M., Ahmadi A., Babajani A., Mazloomnejad R., Hatamnejad M.R., Shariatzadeh S., Bahrami S. and Niknejad H., Immunogenicity of decellularized extracellular matrix scaffolds: a bottleneck in tissue engineering and regenerative medicine, *Biomaterials Research*, **27(1)**, 10 **(2023)**

12. Keane T.J., Swinehart I.T. and Badylak S.F., Methods of tissue decellularization used for preparation of biologic scaffolds and in vivo relevance, *Methods*, **84**, 25-34 **(2015)**

13. Kular J.K., Basu S. and Sharma R.I., The extracellular matrix: Structure, composition, age-related differences, tools for analysis and applications for tissue engineering, *Journal of Tissue Engineering*, **5**, 2041731414557112 **(2014)**

14. Lee J.S., Choi Y.S., Lee J.S., Jeon E.J., An S., Lee M.S., Yang H.S. and Cho S.W., Mechanically-reinforced and highly adhesive

decellularized tissue-derived hydrogel for efficient tissue repair, *Chemical Engineering Journal*, **427**, 130926 **(2022)**

15. Lee S.J., Lee J.H., Park J., Kim W.D. and Park S.A., Fabrication of 3D Printing Scaffold with Porcine Skin Decellularized Bio-Ink for Soft Tissue Engineering, *Materials (Basel)*, **13(16)**, 3522 **(2020)**

16. Ouyang L., Yao R., Zhao Y. and Sun W., Effect of bioink properties on printability and cell viability for 3D bioplotting of embryonic stem cells, *Biofabrication*, **8(3)**, 035020 **(2016)**

17. Reing J.E., Brown B.N., Daly K.A., Freund J.M., Gilbert T.W., Hsiong S.X., Huber A., Kullas K.E., Tottey S., Wolf M.T. and Badylak S.F., The effects of processing methods upon mechanical and biologic properties of porcine dermal extracellular matrix scaffolds, *Biomaterials*, **31(33)**, 8626-8633 **(2010)**

18. Sarmin A.M. and Connelly J.T., Fabrication of Human Skin Equivalents Using Decellularized Extracellular Matrix, *Curr Protoc*., **2(3)**, e393 **(2022)**

19. Schwab A., Levato R., D'Este M., Piluso S., Eglin D. and Malda J., Printability and Shape Fidelity of Bioinks in 3D Bioprinting, *Chemical Reviews*, **120(19)**, 11028-11055 **(2020)**

20. Somasekharan L., Kasoju N., Raju R. and Bhatt A., Formulation and Characterization of Alginate Dialdehyde, Gelatin and Platelet-Rich Plasma-Based Bioink for Bioprinting Applications, *Bioengineering*, **7(3)**, 108 **(2020)**

21. Taneja H., Salodkar S.M., Singh Parmar A. and Chaudhary S., Hydrogel based 3D printing: Bio ink for tissue engineering, *Journal of Molecular Liquids*, **367**, 120390 **(2022)**

22. Thangaraju P. and Varthya S.B., ISO 10993: Biological Evaluation of Medical Devices, in Medical Device Guidelines and Regulations Handbook, Timiri Shanmugam P.S. et al, Editors, Springer International Publishing, Cham., 163-187 **(2022)**

23. Tracy L.E., Minasian R.A. and Caterson E.J., Extracellular Matrix and Dermal Fibroblast Function in the Healing Wound, *Advances in Wound Care*, **5(3)**, 119-136 **(2014)**

24. Vaghela Hiral, Parmar Kokila and Mahyavanshi Jyotindra, Biogenic Synthesis of Gold Nanoparticles using Bark Extract of Bauhinia variegata: Antibacterial and in vitro Anticancer study, *Res. J. Chem. Environ.*, **28(1)**, 48-56 **(2024)**

25. Ventura R.D., Padalhin A.R., Park C.M. and Lee B.T., Enhanced decellularization technique of porcine dermal ECM for tissue engineering applications, *Materials Science and Engineering: C*, **104**, 109841 **(2019)**

26. Wolf M.T., Daly K.A., Brennan-Pierce E.P., Johnson S.A., Carruthers C.A., D'Amore A., Nagarkar S.P., Velankar S.S. and Badylak S.F., A hydrogel derived from decellularized dermal extracellular matrix, *Biomaterials*, **33(29)**, 7028-7038 **(2012)**

27. Xie Z., Gao M., Lobo A.O. and Webster T.J., 3D Bioprinting in Tissue Engineering for Medical Applications: The Classic and the Hybrid, *Polymers (Basel)*, **12(8)**, 1717 **(2020)**

28. Xing H., Lee H., Luo L. and Kyriakides T.R., Extracellular matrix-derived biomaterials in engineering cell function, *Biotechnol Adv*., **42**, 107421 **(2020)**

29. Zhang H., Wang Y., Zheng Z., Wei X., Chen L., Wu Y., Huang W. and Yang L., Strategies for improving the 3D printability of decellularized extracellular matrix bioink, *Theranostics*, **13(8)**, 2562-2587 **(2023)**

30. Zhang X., Chen X., Hong H., Hu R., Liu J. and Liu C., Decellularized extracellular matrix scaffolds: Recent trends and emerging strategies in tissue engineering, *Bioactive Materials*, **10**, 15-31 **(2022)**.

(Received 21th October 2024, accepted 23rd November 2024)